Materials Science and Technology

ISSN: 0267-0836 (Print) 1743-2847 (Online) Journal homepage: https://www.tandfonline.com/loi/ymst20

Laser cladding with (WC+W_2C)/Co–Cr–C and (WC +W_2C)/Ni–B–Si composites for enhanced abrasive wear resistance

R. C. Gassmann

To cite this article: R. C. Gassmann (1996) Laser cladding with (WC+W_2C)/Co–Cr–C and (WC +W_2C)/Ni–B–Si composites for enhanced abrasive wear resistance, Materials Science and Technology, 12:8, 691-696, DOI: 10.1179/mst.1996.12.8.691

To link to this article: https://doi.org/10.1179/mst.1996.12.8.691

Laser cladding with (WC + W_2C)/Co–Cr–C and (WC + W_2C)/Ni–B–Si composites for enhanced abrasive wear resistance

R. C. Gassmann

Composites of three different tungsten carbide powders and two matrix alloys of the Co–Cr–C and Ni–B–Si type were cladded on to mild steel using a 6 kW CO_2 laser. The effects of parameter variation, such as volume fraction of carbides within the matrix, beam intensity, and traverse speed on the coatings' morphology were investigated. Coatings with up to 40 vol.-% unmelted carbides, excellent bonding, and without cracks were obtained. This study has confirmed that, in the area of applying composite materials, laser powder cladding is technologically superior to conventional deposition welding using filler wire.

MST/3409

 Manuscript received 20 July 1995. *The author is at the Fraunhofer Resource Center for Laser Technology, Ann Arbor, MI, USA.*

Introduction

The resistance of a material to abrasive wear is basically governed by its hardness and grain size. In general, as hardness and grain size increase the wear rate decreases.[1] The best abrasive wear performance is achieved with cemented carbides. Carbide components are manufactured by sintering carbide particles, mostly tungsten carbide, with a metallic binder phase, usually cobalt. Owing to the high carbide content of about 75 to 98% and the regular distribution within the structure, the carbide particles govern tribological behaviour while the matrix alloy essentially holds the carbides together and transmits mechanical stresses. For this reason, cemented carbides combine both features, high hardness and large grain size, which are important for wear performance.

Classic sintering techniques; however, cannot be used for applying carbide coatings on to components. Cladding of components with carbidelike materials, which may imply a lower carbide/matrix ratio than that of cemented carbides, can be performed either by plasma spraying or deposition welding. Plasma sprayed coatings, in many applications, do not provide sufficient bonding to the substrate. Conventional arc welding with carbide filled wires is associated with a high energy input, which causes considerable carbide dissolution and the precipitation of brittle phases. With the availability of reliable high power CO_2 lasers, a new deposition welding technique has been developed during the mid 1980s, namely laser powder cladding.[2] Laser powder cladding is distinguished by the generation of a local melt on the substrate surface and pneumatic feed of the coating material into the melt pool. The use of laser radiation enables the variation of both melt temperature and local interaction time over a wide range. Also, the laser cladding process involves less turbulence within the melt than arc welding[3] and, if needed, temperature profiles across the melt pool can be set using beam forming equipment, such as integrating or oscillating mirrors. Thus, carbide dissolution within the melt as well as penetration of the substrate can be controlled accurately.

In the present investigation three tungsten carbide powders with different characteristics were clad with Co–Cr–C and Ni–B–Si matrix alloys in mixtures of up to 50 vol.-% carbide on to mild steel. The purpose of this study was to determine suitable carbide powder morphologies and matrix alloy compositions, maximum carbide contents, and optimal process parameters to achieve low carbide dissolution as well as slight substrate penetration.

Fundamental aspects

The present investigation was based on tungsten carbide, because it is the most widely used hard material in manufacturing cemented carbides. Tungsten carbide (WC) holds a leading position among other carbides since it combines favourable properties, such as high hardness and a low coefficient of thermal expansion, which is $3{\cdot}88–5{\cdot}96 \times 10^{-6}\ K^{-1}$ (273–2000 K, polycrystalline).[4] Also, tungsten carbide is distinguished by a certain amount of plasticity[5] and good wettability by molten metals, particularly cobalt. The main disadvantage of WC is its low heat of formation of about $-40\ kJ\ mol^{-1}$ (Refs. 6 and 7), which makes it easily dissolved by molten metals. The low carbon concentration in matrix alloys, which are commonly used for deposition welding of carbide/alloy composites, and the rapid cooling of the melt cause complex carbide precipitates to form. An example is the metastable and extremely brittle η phase, M_3W_3C. Therefore, carbide dissolution within the melt directly affects the matrix embrittlement, which can be indicated by the matrix hardness. Beyond a critical

Table 1 Characteristics of experimental powders

Powder	Type	Particle size, μm	Composition, wt-%								
			C	Si	Cr	Mo	B	Fe	WC/W_2C	Ni	Co
M1	CoCrC alloy	45–125	0·25	...	27·0	5·50	...	...	...	2·80	Bal.
M2	NiBSi alloy	45–125	0·15	2·18	<1·0	...	1·5	<1·0	...	Bal.	...
C1	WC/Co: Co coated agglomerated	20–50	...	...	...	...	...	...	83·0	...	17·0
C2	WC melt carbide	45–125	...	...	...	...	...	...	100	...	...
C3	WC/Ni melt carbide, Ni coated	25–125	...	...	...	...	...	...	92·0	8·0	...

matrix hardness, the matrix alloy is not able to accommodate shrinkage strains, and cracks occur during cooling.

In general, there are two methods of preparing tungsten carbide, which are important for production on an industrial scale: carburisation of elemental tungsten powder and eutectic melting of tungsten and carbon to form melt carbide. The melt carbide possesses higher hardness as well as higher density.[8] Hence, tungsten melt carbide is preferred in manufacturing cemented carbide and for wear protection purposes. In the W–C system, three eutectic reactions occur and tungsten carbide exists in three intermediate phases, namely W_2C, α-WC_{1-x}, and WC with W_2C undergoing polymorphic transformation. The equiatomic WC is formed peritectically at 2776°C and 6·13 wt-% (50 at.-%) and has a narrow homogeneity range,[6] which also decreases with temperature. When producing fused tungsten carbide, a eutectic melt of about 4·5 wt-% (42 at.-%) carbon is rapidly cooled, yielding a mixture of WC and W_2C. At carbon contents above 4·5 wt-%, graphite precipitates which reduces hardness and wear resistance substantially. Carbon contents below 3·8 wt-% (38 at.-%) yield high quantities of W_2C. Structures dominated by ditungsten carbide, however, are inappropriate for wear applications since the W_2C phase is extremely brittle and is chemically as well as tribologically less resistant than the monocarbide.

Experimental

Three tungsten carbide powders with different manufacturing histories and/or metal coatings were chosen in order to determine the carbide dissolution dependence on the particle morphology. The characteristics of the experimental carbide powders are given in Table 1. Powder C1 was manufactured by carburising tungsten powder and subsequent agglomeration with 17 wt-%Co. The tungsten carbide had a small particle size of less than 6 μm. The particle size of the agglomerated powder used in the experiments was about 20–50 μm (Fig. 1*a*). Powder C2 was coarse melt carbide without metal coating. The particles exhibited a typical melt carbide structure of WC needles within a W_2C matrix, as shown from the polished cross-sectional surfaces in Fig. 1*b*. It is also shown from Fig. 1*b* that the structures of the centred particles are coarse compared with those of the particles at either side. This suggests that the cooling rate during manufacturing the powder was not homogeneous. Powder C3 was also melt carbide, but with a nickel coating. Optical microscopy of polished cross-sections of such particles (Fig. 1*c*) shows that the thickness of the nickel coating varied considerably along the perimeter. Since areas within the particles, which seem associated with WC crystals, appear just as bright as the nickel coating, it is assumed that the nickel partially diffused into the carbide.

The chemical compositions of the matrix alloys used are given in Table 1. The selection was guided by two objectives. First, one cobalt base and one nickel base alloy were chosen in order to determine differences in the kinetics of carbide dissolution in cobalt and nickel melts. Second, hardfacing alloys with the lowest nominal hardness available were used in order to prevent cracking. Hence, both alloys contained little carbon. Since preliminary studies had shown that chromium and boron form very brittle phases in NiCrBSi alloys, a nickel base alloy (M2) with small amounts of chromium and boron was chosen.

The experimental setup is illustrated schematically in Fig. 2. All experiments were carried out with a Rofin Sinar RS 6000 CO_2 laser (TEM_{20}). The power output was kept constant at 5·0 kW. The beam was focused by a parabolic mirror. The mean beam intensity within the spot was alternately set to 0·9, 1·2, 1·6, and $2{\cdot}3 \times 10^4$ W cm^{-2} by changing the working distance from the focal plane. Mixtures of 12·5, 20, and 40 vol.-% of the three different carbide powders within the M1 matrix alloy and of 40 and 50 vol.-% of the C2 powder within the M2 matrix were prepared and continuously fed into the melt pool by an argon gas stream. Mild steel (0·15 wt-%C) specimens of 10 mm height, 100 mm length and 60 mm width served as the substrate. By moving the specimens at traverse speeds

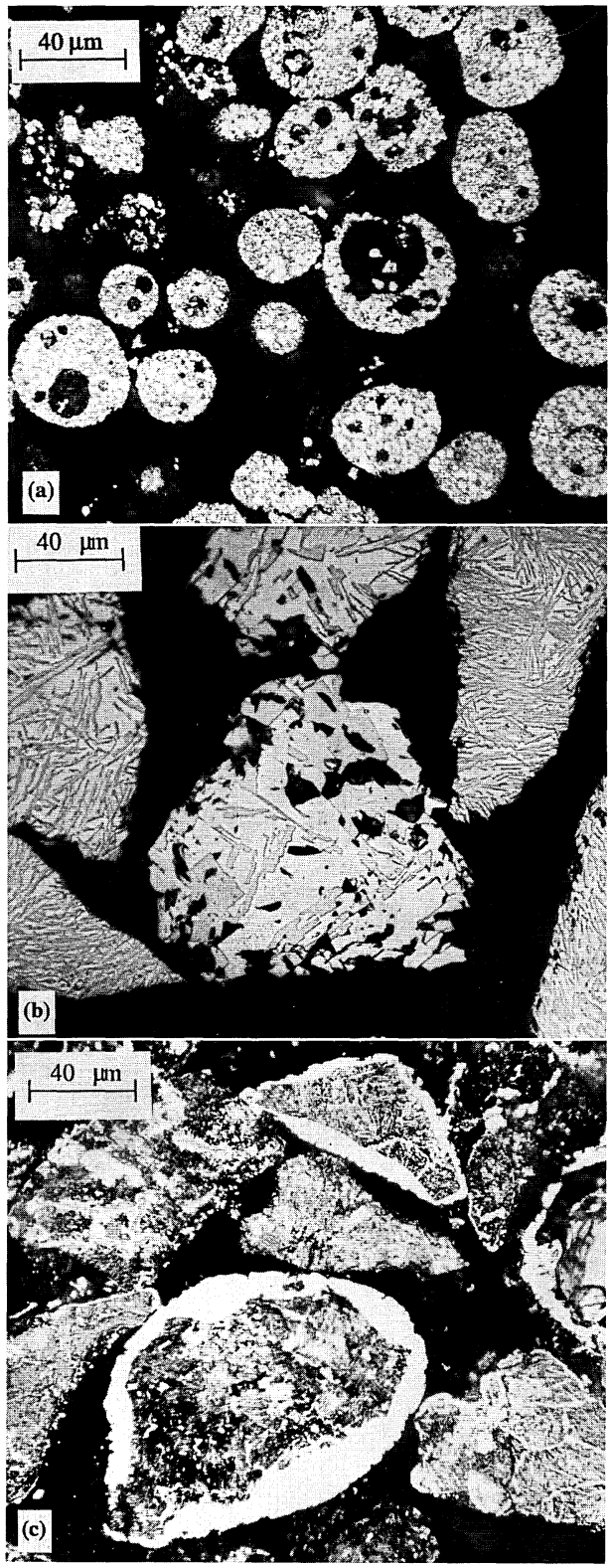

a C1; *b* C2; *c* C3

1 Micrographs of polished particles of tungsten carbide powders

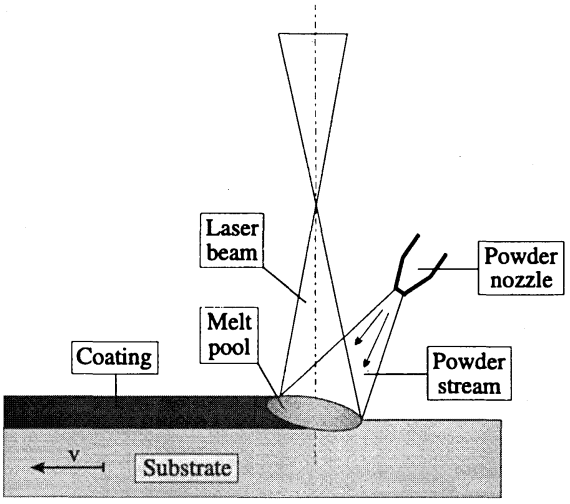

2 Schematic diagram of experimental setup

between 100 and 600 mm min^{-1}, tracks of 70 mm length were generated. The powder feed rate was set up in such a way that the width/height ratio of a single track ranged between 4 and 6. By overlapping a minimum of five tracks, coatings were produced.

Results and discussion

CLADDING WITH Co–Cr–C (M1) AND TUNGSTEN CARBIDE (C1, C2, C3)

The M1 matrix alloy could be applied easily with all three carbide powders in each of the prepared mixtures. The single tracks obtained had widths between 5 and 7 mm and single tracks as well as coatings were well bonded to the substrate.

It has been found that the rate of carbide dissolution depends upon the particle size, the existence of a metal coating on the carbide particles, the temperature of the melt, the time the particles stay in the melt, and the main elemental constituent of the melt. The highest carbide dissolution was observed for the C1 powder. The carbide particles were almost completely dissolved at all parameter settings, as seen in the micrograph of a single track (Fig. 3). Blowholes in the agglomerated particles (Fig. 1*a*) also caused pores within the solidified structure (Fig. 3). The dissolution of the C3 carbide was found to be less than that of the C1 powder, but still unsatisfactory high. The

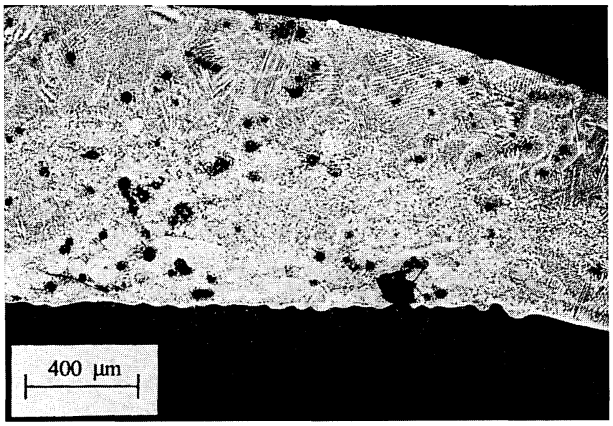

3 Cross-section of M1–12·5 vol.-%C1 single track applied at $0{\cdot}9 \times 10^4$ W cm^{-2} intensity and 0·84 s interaction time

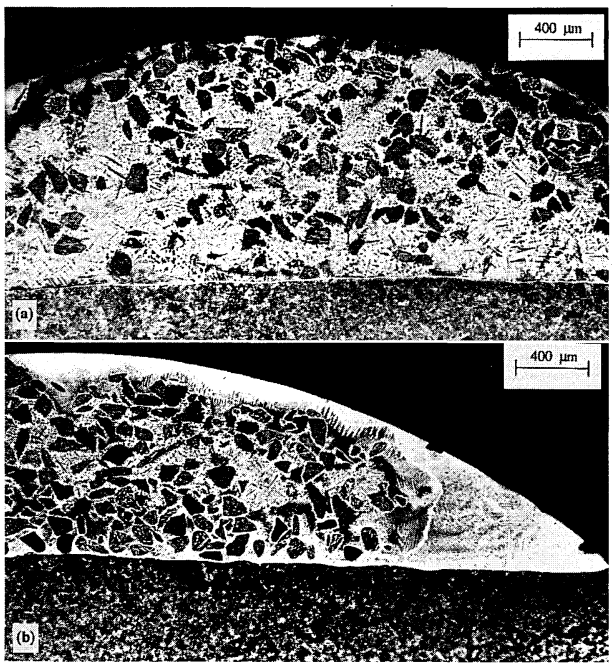

a 20 vol.-%C2; *b* 40 vol.-%C2

4 Cross-sections of M1–C2 single tracks applied at $1{\cdot}2 \times 10^4$ W cm^{-2} intensity and 0·84 s interaction time

lowest carbide dissolution was observed for the pure melt carbide, C2 (Fig. 4). Even the tracks applied at a mean beam intensity of $2{\cdot}3 \times 10^4$ W cm^{-2} and at an interaction time, in the middle of the melt pool, of about 4 s showed a considerable amount of unmelted carbide particles more than 100 μm long within the microstructure. This suggests that a metal coating, intended to improve the particle wettability, substantially increases the rate of carbide

a 20 vol.-%C2; *b* 40 vol.-%C2

5 Optical micrographs of M1–C2 structures (taken from tracks seen in Fig. 4)

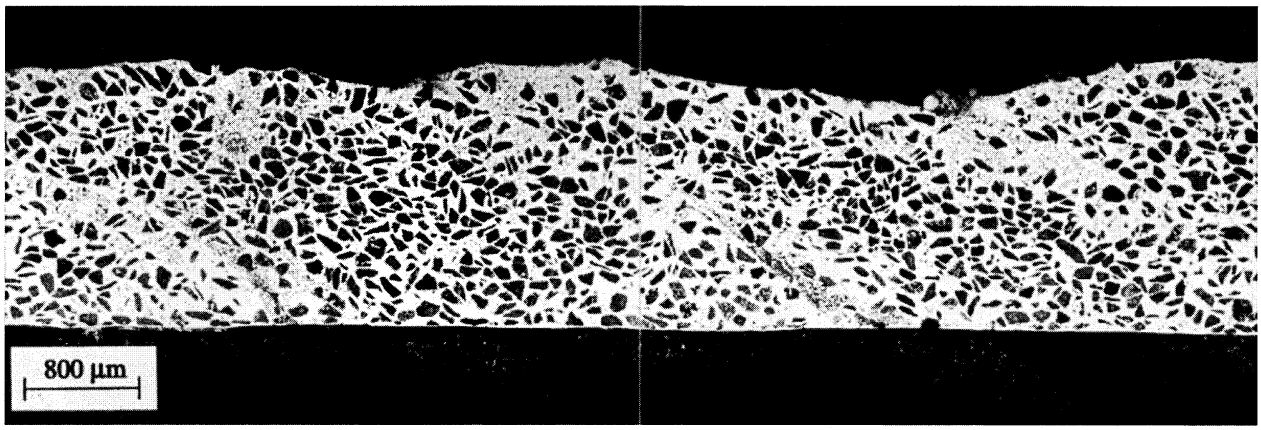

6 Cross-section of M2–40 vol.-%C2 coating produced by overlapping tracks

dissolution. In the case of the C1 powder, the particles consisted of very small core particles surrounded by cobalt as a result of agglomeration. This carbide morphology drastically increased the kinetics of particle dissolution within the melt, resulting in little unmelted carbide. The variation in carbide dissolution rate of the C1 and C3 powders must be attributed to more than the difference between the nickel coating and the cobalt coating. The decreased dissolution of the C3 powder resulted from the coarser particle size and the higher density of the melt carbide. If, as assumed, nickel diffused into the tungsten carbide during coating of the C3 powder, this also may have caused faster carbide dissolution.

Figures 4 and 5 show micrographs of polished and etched cross-sections of two C2/M1 single tracks. The micrographs in Fig. 5*a* and *b* exhibit the same structures as shown in Fig. 4*a* and *b*, respectively, but at higher magnification. During preparation of the specimens, the W_2C phase was selectively etched away from the included carbide particles, and the WC phase was exposed. This resulted in the appearance of WC needles surrounded by dark or blurred regions (Fig. 5*b*). Despite the absence of a metal coating, the C2 carbide was properly wetted. The 20 vol.-% carbide track contained a homogeneous distribution of the carbide particles whereas the 40 vol.-% carbide track exhibited an accumulation of carbide particles in the central area. The higher number of unmelted particles is hypothesised to restrain the Maragoni convection within the melt and block their transportation to the remote edges of the track cross-section. Although both tracks (in Fig. 5*a* and *b*) were applied with identical laser process parameters, the 20 vol.-% carbide structure in Fig. 5*a* (also Fig. 4*a*) exhibits a substantially higher carbide dissolution rate than the 40 vol.-% carbide structure in Fig. 5*b* (also Fig. 4*b*) indicated by precipitated carbides along the particle/matrix boundaries and also by dendrites, which appear dark in a predominantly bright matrix. The 40 vol.-% carbide track, however, exhibits neither initial particle dissolution nor precipitated carbides within the matrix. This suggests that lower temperature and shorter interaction time near the track edges, where the micrograph in Fig. 5*b* was taken, may cause substantially less carbide dissolution than in the track centre, where the micrograph in Fig. 5*a* was taken. A reasonable conclusion is that higher turbulence within the 20 vol.-% carbide melt has resulted in an increase in carbide dissolution since the amount of precipitated carbides was generally higher in the 20 vol.-% carbide structures than in the 40 vol.-% carbide tracks.

The hardness of the single tracks as well as the hardness of the coatings was found to depend predominantly upon the rate of carbide dissolution, but also upon the traverse speed. Microhardness of 2050 to 3080 HV0·05 were measured for carbide particles embedded in the coatings. These numbers are in good agreement with the hardness of WC (~2080 HV) and W_2C (~3000 HV). At tracks of low carbide dissolution, mean matrix hardnesses between 640 and 780 HV0·05 were determined. However, the hardness of the M1 alloy, laser clad without tungsten carbide, usually ranges between 320 and 400 HV, as known from previous studies. This suggests that, even in structures that had been optically identified to have a low carbide dissolution, a considerable amount of hard phases precipitated. In tracks of high carbide dissolution, matrix hardnesses of up to 1150 HV0·05 were measured. As the traverse speed increased from 200 to 500 mm min^{-1}, the mean matrix hardness increased by 30 to 80 HV.

Despite the ductility of the cobalt alloy M1, which is comparable with that of Stellite 21, cracks occurred. The crack rate (Table 2) was dependent upon the carbide content within the powder, the matrix embrittlement (hardness), and the rate of substrate penetration. At high beam intensities and low traverse speeds, no cracks occurred because of the deep substrate penetration (e.g. 1·6 mm at $2{\cdot}3 \times 10^4$ W cm^{-2} and 200 mm min^{-1}). Although carbide dissolution was intense at these parameters, the matrix hardness did not exceed the critical amount as a result of the high iron content and the high melt/particle volume ratio. The crack rate increased with decreasing beam intensity and increasing traverse speed (Table 2). This effect is attributed mainly to less substrate penetration and a lower iron concentration within the melt. On further intensity reduction and increase in speed, iron concentration became insignificant and the effect of reduced carbide dissolution became dominant; therefore, cracks diminished in number.

CLADDING WITH Ni–B–Si (M2) AND TUNGSTEN CARBIDE (C2)

Based on the experiences of the first experimental series, the nickel alloy (M2) was only clad with C2 tungsten melt carbide in mixtures of 40 and 50 vol.-% C2 within the M2. Dissolution of the carbide particles was substantially less than in the cobalt melt. For tracks made from 40 vol.-% carbide powder, the variation of the beam intensity between

Table 2 Average number of cracks in M1 matrix single tracks containing 20(40) vol.-%C2 over 70 mm track length

Mean beam intensity, W cm^{-2}	Traverse speed, mm min^{-1}			
	200	300	400	500
2·3	0(0)	0(0)	0(3)	6(9)
1·6	0(0)	1(7)	10(12)	16(16)
1·2	0(8)	11(10)	10(11)	9(14)

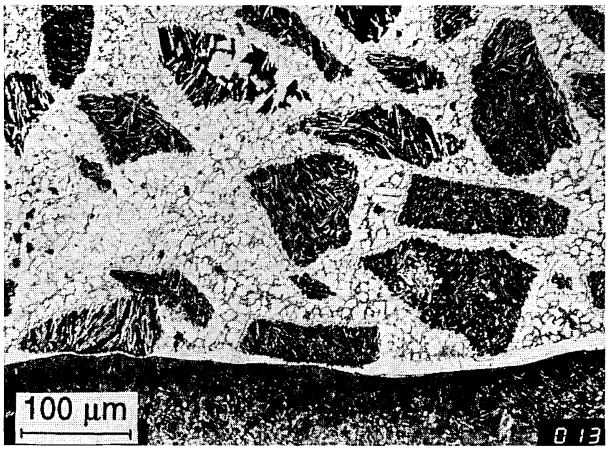

7 Etched microstructure of a M2–40 vol.-%C2 coating

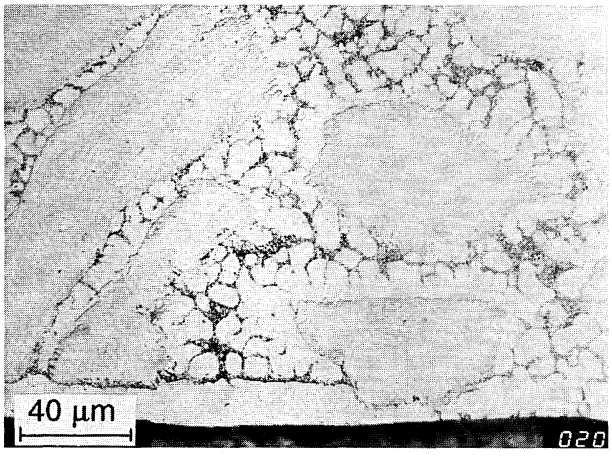

8 Unetched microstructure of a M2–40 vol.-%C2 coating adjacent to the substrate interface

1·6 and 2·3 × 10^4 W cm^{-2} did not affect carbide dissolution and substrate penetration significantly. The increase of interaction time from 0·84 to 1·8 s, however, caused considerable dissolution of the carbide particles, as seen in micrographs.

Coatings produced by overlapping tracks exhibit metallurgical bonding to the substrate as well as at the track interfaces (Fig. 6). The carbide particles are close packed in the cross-sectional area of the tracks. At track interfaces, the number of carbide particles decreases slightly. The carbide particles have been wet properly by the melt at all parameter settings (Figs. 7 and 8). Bonding or wetting defects such as pores along the particle boundaries have not been observed. The carbide particles included in the Ni–B–Si structure exhibit a 2–3 µm thick nickel diffusion zone at their surface, which appears bright in micrographs of polished and etched specimens (Figs. 7 and 9). This diffusion zone has not been observed at particles included in the Co–Cr–C alloy since cobalt, when diffusing into tungsten carbide, instantaneously dissolves the carbide.

The matrix hardness did not indicate carbide dissolution as observed for the cobalt alloy (Table 3). Although remarkable particle dissolution appears from micrographs of tracks applied at low traverse speeds, no major hardness increase has been determined with decreasing traverse speed. Also, no cracks have been observed in any of the M2/C2 specimens. This suggests that even at long interaction times a critical quantity of hard phases does not form due to low carbide dissolution and the absence of chromium.

The increase of the carbide content to 50 vol.-% decreased the viscosity of the melt significantly. The best process parameters found for the 40 vol.-%C2 powder resulted in a strong mass concentration occurring in the track centre. Only increasing the beam intensity above 2·0 × 10^4 W cm^{-2} and reducing the traverse speed to 200 mm min^{-1} yielded regularly shaped tracks. In these tracks a considerable amount of the carbide particles were dissolved so that the absolute quantity of unmelted particles remained less than in tracks of 40 vol.-%C2 powder.

Table 3 Matrix hardness of M2–40 vol.-%C2 coatings: minimum–average–maximum

Mean beam intensity, W cm^{-2}	Traverse speed, mm min^{-1}		
	200	300	400
1·6	367–452–512*	...	...
	364–430–498	...	...
1·9	...	336–417–473	...
2·3	...	...	322–441–561

* Single track.

Conclusions

This study has determined coarse melt carbide with a particle size between 45 and 125 µm to be the superior carbide morphology for applying tungsten carbide/metal composites for enhanced abrasive wear resistance. Cobalt or nickel coated tungsten carbide must be avoided in order to prevent excessive carbide dissolution within the melt. Coated carbide particles are not essential either, since tungsten carbide is easily wetted by nickel and cobalt melts. Particle sizes larger than 125 µm were not investigated, nevertheless it is assumed that carbide particles up to 150 µm can be used. A carbide level of 40 vol.-% within the matrix alloy is the highest that can be applied without major technological difficulty, such as insufficient melt viscosity. Coatings containing 40 vol.-% carbide also exhibit equivalent resistance to abrasive wear as traditionally cemented carbides.[9] Hence, 40 vol.-% unmelted carbide within the coating is a functional limit as well, and higher carbide levels are not required.

Selection of a proper matrix alloy requires two considerations: the impact of the base metal on carbide dissolution and the potential for the formation of brittle phases with components of the dissolved carbide. Nickel alloys do not dissolve tungsten carbide as rapidly as cobalt alloys do, hence tungsten carbide/nickel composites can be applied under a relatively broad range of processing parameters, particularly beam intensity. This becomes advantageous when cladding sites of reduced heat conduction through

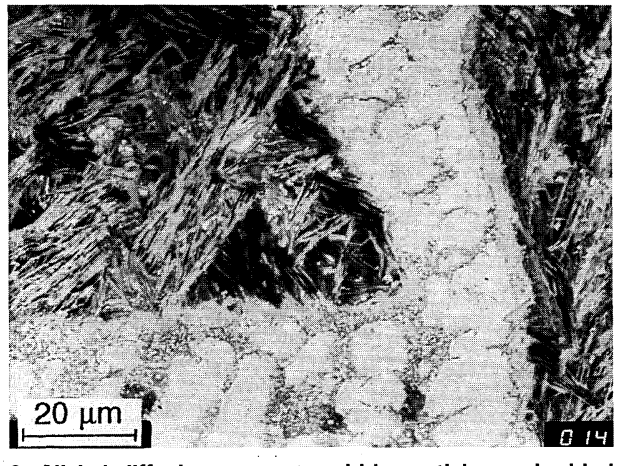

9 Nickel diffusion zone at carbide particles embedded in Ni–B–Si (C2) matrix alloy

the substrate as a result of complicated component shape or simply low conductivity of the substrate material. In order to prevent precipitation of brittle hard phases, alloys with low contents of carbon, boron, and chromium, such as alloy M2, should be used. The low hardness of these alloys does not increase the wear rate of the coating. On the contrary, as the matrix hardness decreases both the wear rate and the probability of cracking also decrease.[1] A ductile matrix is more able to hold on to the carbide particles adjacent to the surface and prevent them from tearing out during abrasive wear, than a hard matrix. The occurrence of cracks depends upon the kind and quantity of precipitated hard phases within the matrix. In general, a matrix hardness which is substantially less than 600 HV has to be achieved in order to prevent cracking.

Coatings of 40 vol.-%C2 (tungsten melt carbide) within the Ni–B–S alloy (M2) exhibiting excellent properties have been bonded on to steel using a simply focused 5 kW CO_2 laser beam at mean intensities in the spot of between 0·95 and $2{\cdot}3 \times 10^4$ W cm^{-2} and interaction times at the track centre between 0·8 and 1·6 s. The cladding rate for these parameters was 5 cm^2 min^{-1} for a usable coating thickness of 1·5 mm and 9 cm^2 min^{-1} for a coating thickness of 1 mm. The Co–Cr–C alloy (M1) has been clad with best results in mixtures with 40 vol.-%C2 (tungsten melt carbide) at mean beam intensities between 1·2 and $1{\cdot}6 \times 10^4$ W cm^{-2} and an interaction time of about 0·8 s at the track centre. For some applications of cladding cobalt matrix/tungsten carbide composites, the use of beam forming equipment which generates rectangular melt pools with low temperature gradients across the melt pool may be necessary in order to avoid excessive carbide dissolution.

Acknowledgement

The author would like to thank Donald F. Heaney from the Department of Materials Science at The Pennsylvania State University for his review of this paper.

References

1. K. J. BHANSALI and W. L. SILENCE: *Met. Prog.*, 1977, **11**, 39–43.
2. R. C. GASSMANN: PhD dissertation, Dresden, Germany, 1990.
3. S. ATAMERT and H. K. D. H. BHADESHIA: *Metall. Trans. A*, 1989, **20A**, (6), 1037–1053.
4. Y. S. TOULOUKIAN, R. K. KIRBY, R. E. TAYLOR, and T. Y. R. LEE: 'Thermophysical properties of matter', Vol. 13, 'Thermal expansion of nonmetallic solids'; 1970, New York, Washington, IFI/Plenum Press.
5. D. J. ROWCLIFFE, V. JAYARAM, M. K. HIBBS, and R. SINCLAIR: *Mater. Sci. Eng.*, 1988, **A105–106**, (1–2), 299–303.
6. S. V. NAGENDER NAIDU, A. M. SRIRAMAMURTHY, and P. RAMA RAO: 'Phase diagrams of binary tungsten alloys'; 1991, Calcutta, Indian Institute of Metals.
7. T. IAWA, I. TAKAHASHI, and M. HANDA: *Metall. Trans. A*, 1986, **17A**, (11), 2031–2034.
8. R. HAHN, E. LUDERITZ, S. SATTELBERGER, and H. J. RETELSDORF: *Metall.*, 1986, **40**, (10), 1009–1011.
9. R. C. GASSMANN, St. NOWOTNY, A. LUFT, and W. REITZENSTEIN: in Proc. Int. Conf. on 'Applications of lasers and electro optics', Orlando, FL, USA, October 1993, Laser Institute of America, 288–300.